Article

Not peer-reviewed version

Increasing Efficiency in Tertiary Buildings through PoE LVDC Nanogrid in the island of La Réunion

Olivia Graillet *, Denis Genon-Catalot, Pierre-Olivier Lucas de Peslouan, Flavien Bernard, Frédéric Alicalapa, Laurent Lemaitre, Jean-Pierre Chabriat

Posted Date: 2 February 2024

doi: 10.20944/preprints202402.0110.v1

Keywords: lvdc nanogrid; energy efficiency; power over ethernet; solar energy; line losses; building

Article

Increasing Efficiency in Tertiary Buildings through PoE LVDC Nanogrid in the Island of La Réunion

Olivia Graillet [1,3,*], Denis Genon-Catalot [2], Pierre-Olivier Lucas de Peslouan [1], Flavien Bernard, [1,3], Frédéric Alicalapa [1], Laurent Lemaitre [3] and Jean-Pierre Chabriat [1]

1 University of La Réunion, ENERGY-Lab, 97490 Saint-Denis, La Réunion, France
2 University of Grenoble Alpes, Grenoble INP, LCIS, 26000 Valence, France
3 Intégrale Ingénierie, 97435 Saint-Gilles-les-Hauts, La Réunion, France
* Correspondence: olivia.bory-devisme@univ-reunion.fr

Abstract: In the context of the French tertiary decree, it is crucial to reduce the energy consumption of buildings by first addressing the design of the electrical architecture. Implementing Direct Current (DC) nanogrids in buildings could offers a promising advantage for energy efficiency, significantly impacting overall energy consumption and sustainability goals. For an insulated area with a subtropical climate, such as La Réunion island, DC nanogrids could also facilitate the insertion of local renewable energy sources, especially solar energy. This article presents the deployment and efficiency evaluation of an end-to-end Low Voltage Direct Current (LVDC) nanogrid, from conception to real-world installation within a company. The nanogrid consists of a photovoltaic power plant, a Lithium-Iron-Phosphate (LFP) battery, and DC end-use equipment such as LED lighting and DC fans for two individual offices. An innovation is provided for the power supply and energy management of terminal equipment using the Power Over Ethernet (PoE) standard IEEE 802.3bt. The efficiency of the nanogrid is measured to be 40% higher than the efficiency of an installation powered by PV and distributed at 230 VAC. These results are obtained under certain deployment conditions, which are discussed in this article, in order to enhance the energy efficiency of buildings by using 48VDC. The nanogrid hardware and software infrastructure, the methodology employed for efficiency quantification and the measurement results are described in the paper.

Keywords: LVDC nanogrid; energy efficiency; power over ethernet; solar energy; line losses; building

1. Introduction

In the context of global energy transition, it is essential to reduce the carbon impact of buildings, from the design phase through to the operational phase. During operation, the building's carbon impact will first depend on the primary energy source used to supply electricity and secondly on the building's electricity consumption, which in turn will depend on the chosen electrical architecture, the efficiency of terminal equipment and user behavior.

In response to these challenges, the French government has published the tertiary sector decree [1] and the Building Automation and Control System (BACS) decree [2]. The aim of the first decree is to reduce the energy consumption of commercial buildings by 40% in 2030, by 50% in 2040 and 60% in 2050. The aim of the second decree is to instrument buildings to monitor energy savings achieved or to be improved. Another government objective is for non-interconnected zones, including La Réunion island, to achieve energy autonomy by 2030 [3]. Indeed, the island which is a French overseas department located in the south-western part of the Indian Ocean, is currently 69% dependent on fossil fuels [4]. Concerning the local energy impact of buildings, they account for 86% of annual electricity consumption [5]. The local annual solar radiation is between 1100 and 2100 kWh/m², and the territory can experience cyclonic phases including power cuts. Promoting the development of solar energy while reducing the energy consumption of buildings appears to be a lever of action to contribute to the energy autonomy of the department.

 doi:10.20944/preprints202402.0110.v1

Micro and nanogrids, which are small-cale electrical grid, are currently highlighted due to their ability to facilitate renewable energies penetration. They include one or more energy sources, often renewable, a storage system and an intelligent energy management system. They can operate connected to the grid or in island mode, disconnected from the grid [6]. Microgrids could be particularly well suited for an island such as La Réunion, which needs to achieve energy autonomy.

End-to-End Direct Current (DC) microgrids use direct current electricity from the production to the final equipment. They have the distinct advantages of reducing the need for power converters and shortening energy transmission distances. They are considered to be one of the primary solutions for energy savings according to several studies [6–15].There are even communities, such as those in the USA, that live comfortably and daily on 100% DC microgrids [16]. Despite these promising estimates, a major challenge lies ahead for the industrial sector, as electrical equipment manufacturing norms and standards need to evolve if DC installations are to be democratized on a large scale [17]. The costs of DC circuit breakers and appliances are currently still high. Additional studies and feedback are necessary to guide legislative writings and industrial developments. Otherwise, concerning the scientific challenges, the number of experimental sites needs to grow, to confirm or not the estimates predominantly based on simulations. The results require real data to validate or refute hypotheses regarding the efficiency of micro and nanogrids [17–20].

As points of comparison in the department of La Réunion, microgrids have already been deployed in isolated sites such as the Cirque of Mafate [21,22]. The houses located on this site have the particularity of being completely disconnected from the electrical grid. Each maintenance intervention on the equipment requires helicopter transportation, which has an impact in terms of cost and carbon impact. Finding sustainable solutions for remote control and strategies aimed at preserving the lifespan of the installed equipment is therefore essential.These microgrids utilize solar energy as the primary energy source and lithium-ion batteries for energy storage, or hydrogen storage for hybrid sites [21]. When solar power generation is insufficient, users resort to fuel generators. The electricity is then distributed to households in alternating current (AC), in order to respect current norms and to be fitted with final commons equipments like washing machines and televisions. As can be seen in the electrical architecture of the hybrid site [21], the 48VDC bus is used at the output of the battery and the hydrogen system, before being converted to 230VAC for the buildings. According to [23] and [24], the 48VDC distribution bus is the most suitable in terms of costs and efficiency for deployments over short distances in buildings. Given the reduced distances for electricity distribution in microgrids, it therefore seems pertinent to experimentally study the advantages and limitations of 48VDC distribution. Finally, regarding the other microgrid example [22], the contribution is focused on energy management, through a user interface. Energy gains of 22% were measured, in the scenario where the user follows the recommendations of the user interface as much as possible. It therefore seems relevant to associate energy management with 48 VDC distribution to maximize the performance of a nanogrid.

In the Indian Ocean sector, other microgrids have been deployed and are operational in Madagascar [25]. In their case, the distribution buses used are exclusively in direct current; a 60 VDC bus connects several nanogrids, and within the dwellings, 12, 24, or 48 VDC buses are used depending on the application cases.

These different examples concern the residential sector, but in the case of the deployment presented in this article, a focus is made on an application case in the tertiary sector. According to M. Uddin et al [27], microgrids are currently facing several technical challenges such as "operation, component and compability, integration of distributed energy resources and protection". In this paper, firstly, a contribution regarding the "component and compatibility" challenge is provided. The presented hardware and software architecture allows for experimental feedback on the communication protocols used for the instrumentation and supervision of the DC nanogrid. Secondly, the efficiency of the DC nanogrid is assessed using a methodology for calculating voltage drops, and the values are compared with experimental measurements using a test bench. The DC measurements are compared to a DC/AC/DC distribution, which corresponds to current solar energy installation in buildings.

 doi:10.20944/preprints202402.0110.v1

The article is organized as follows: Section 2 presents the LVDC Nanogrid deployment and details the hardware and software choices. Section 3 outlines the methodology used to theoretically evaluate the efficiency of the nanogrid. Section 4 compares the theoretical results with the experimental measurements taken on site. Finally, Section 5 summarizes the conclusions and outlooks of this work.

2. LVDC Nanogrid Deployment

The building studied is an engineering firm made up of around fifty employees with working hours of between 8AM and 6PM on average. The building is west oriented and the surface area of the premises is 590 m². The energy consumption of the premises is constantly monitored by category of equipment (air conditioning, lighting, ventilation, computer equipment, electric vehicle charging stations and other sockets).

The premises consumed 83 kWh/m² in 2022, and the breakdown of energy consumption showed that direct current appliances, which are led lighting, EV charging and computer equipments accounts for 42% of the total electricity consumption. This percentage highlights the fact that direct current has a larger share in the tertiary sector than in the residential sector, given the amount of IT equipment. It is therefore a lever for optimizing the overall energy reduction of buildings.

Two individual offices have been identified on the company premises to serve as demonstrators. The nanogrid distribution rack is located in the technical room, approximately 25 meters in cable distance from the two offices. Figure 1 localizes the implementation of the nanogrid deployment on the island and in the building.

Figure 1. (a) Localization of the company on the west coast of the island. (b) Photo of the building where the nanogrid is deployed. (c) Highlighted location of the premises, located on the 3rd floor. (d) Localization of the two individual offices used for the DC nanogrid deployment, located at 25m from the power rack.

2.1. Hardware Architecture - 48 VDC Distribution

The LVDC nanogrid has a 3 kWp photovoltaic power station, installed on the sloped roof of the building. In order to correlate the external meteorological condition data with the internal energy production and consumption data and thermal comfort, a solar and meteorological station has also been installed on the roof, photographed in Figure 2.

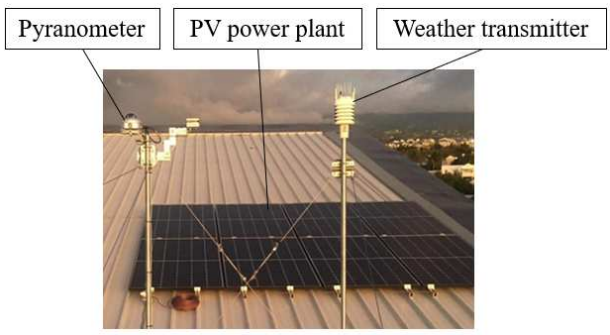

Figure 2. Photo of the 3 kWp PV power plant and weather station on the roof.

 doi:10.20944/preprints202402.0110.v1

The output voltage is regulated to 48 VDC by an MPPT (Maximum Power Point Tracker) regulator. The 48 VDC distribution bus can then be powered: either by the PVs, or by a 2.4 kWh capacity Lithium-Iron-Phosphate battery, or by the grid through an inverter. In the studied case, the grid is not used as a power source, as the nanogrid is totally disconnected from the grid. The inverter is installed to conduct efficiency tests, either in DC/AC/DC architecture or in a completely end-to-end DC architecture. Figures 3 and 4 show respectively the distribution rack of the DC nanogrid and the block diagram with the components.

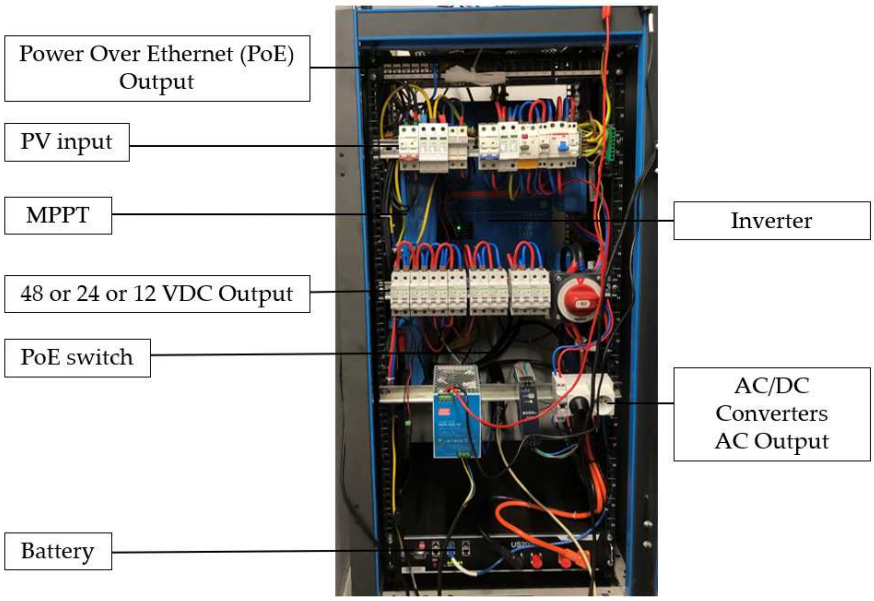

Figure 3. Photo of the power rack distribution of the LVDC nanogrid.

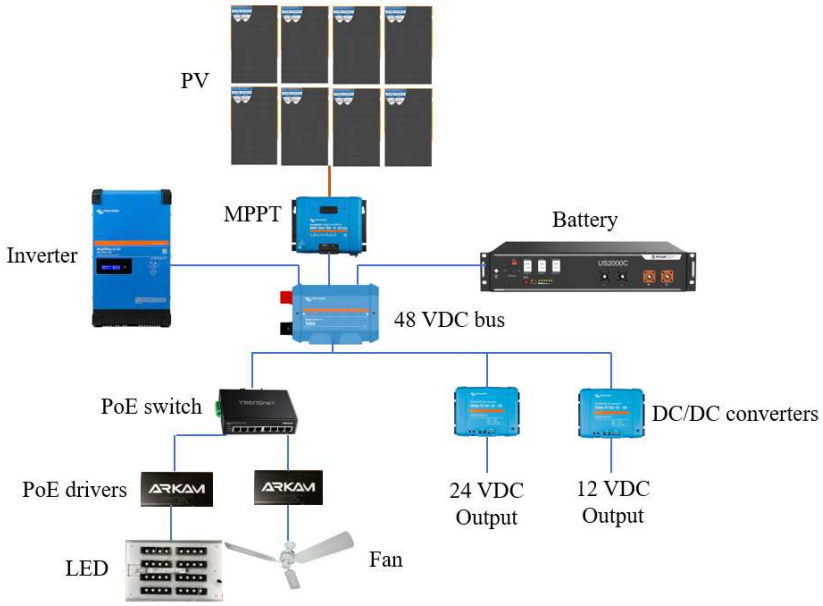

Figure 4. Block diagram including the LVDC nanogrid components.

The protective elements are not detailed in the context of this article, but they consist of a DC circuit breaker adapted to the caliber of the equipment. During the measurement phases, these circuit breakers allow for switching on or tripping the various components connected to the 48VDC bus.

 doi:10.20944/preprints202402.0110.v1

The nanogrid is supplemented by 48/24VDC and 48/12VDC to power equipment that requires these distribution buses, such as the weather station (24VDC).

The Power Over Ethernet (PoE) technology is chosen for the energy distribution and the control of the terminal equipment. Indeed, it operates natively at 48 VDC. The main advantage is to use only a single RJ45 cable for electrical power and to provide internet network to the equipment. The maximum power allowed for the 802.3bt protocol being 100W, the terminal equipment used in this architecture are LED panels (max 35 W) and DC fans (max 20 W). As a point of comparison with other LVDC nanogrids, in the "DC nanogrid house" [26] PoE is used to power indoor environmental sensors. All the other communication protocols used to retrieve all the measurements from the nanogrid are detailed in the following section.

2.2. *Software Architecture*

2.2.1. Communication protocol

All components of the nanogrid are interconnected. The communication links are depicted in Figure 5.

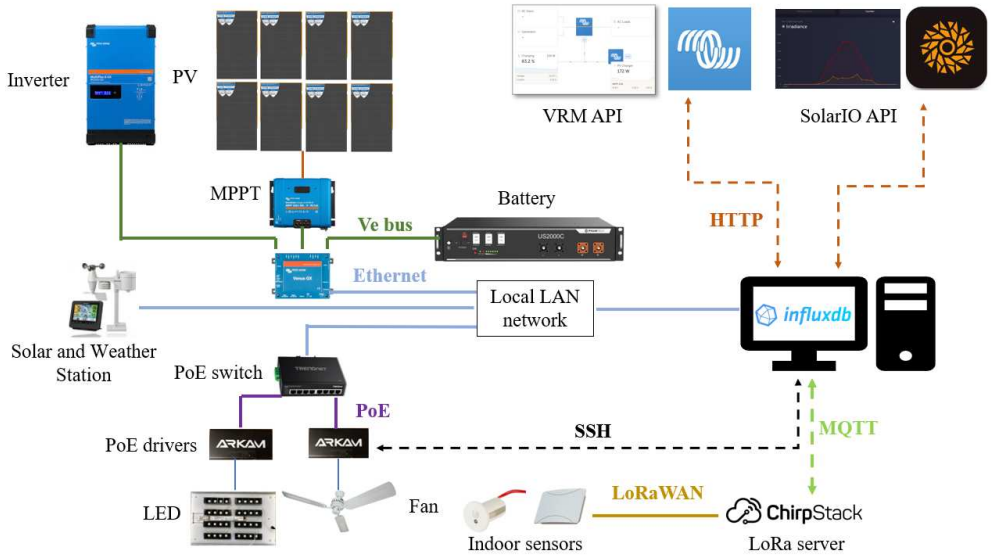

Figure 5. Communication protocols of the DC nanogrid

Pertaining to the energy production and storage segment, the MPPT regulator, inverter, and battery are linked via a Ve.bus communication to a gateway, which is connected to the local internet network. The data, such as voltage (V), current (A) and power (W), measured and recovered by the gateway are subsequently transmitted to a user interface termed "VRM" provided by the manufacturer.

The solar and meteorological station is integrated into the IOS-net network of stations overseen by the ENERGY-Lab laboratory. As a result, open data are transmitted in near real-time to both a web and mobile application [29].

Both the VRM application and the SolarIO application have an associated Application Programming Interface (API). Information is retrieved using the Hypertext Transfer Protocol (HTTP) communicating with their respective APIs.

For the PoE drivers, each device has an Internet Protocol (IP) address. As a result, it is feasible to retrieve voltage (V), current (A), and power (W) information by querying the drivers via Secure Socket Shell (SSH) communication. The PoE drivers have two possible power supply options: either a direct PoE supply or a 48VDC power input combined with an ethernet input. The driver has three possible outputs: two for 48 VDC loads, with a maximum of 1A, and one serial output for communication with

 doi:10.20944/preprints202402.0110.v1

a sensor. In our setup, a luminosity and presence sensor is connected to the driver, allowing for local lighting regulation based on user presence and ambient light levels.

2.2.2. Human Machine Interface (HMI)

Currently, the existing instrumentation of electrical equipment within the enterprise is segmented into multiple user interfaces: one for air conditioning, another for general energy consumption, one for lighting management, one for electric vehicle charging stations, another for environmental indoor IoT (Internet of Things) sensors, and a final one for the weather station. Specifically for lighting, dimming is set using the DALI (Digital Addressable Lighting Interface) protocol and controlled via a mobile application, but the measurements are not usable. In the case of fan units, the user controls them manually, using remote controls. The entirety of these interfaces or platforms does not allow for data retrieval for subsequent processing. When it does, it's typically in the form of .csv files that can be manually extracted. This procedure requires numerous hours of work for data analysis made by energy management engineers in the company.

In the case of the LVDC nanogrid deployed for this project, the advantage of using electrical equipment connected to the network or equipped with a dedicated API greatly simplifies data processing. Particularly with PoE technology for certain equipment, the main advantage is that it can supply power and at the same time collect, control and analyze measurement data from equipment via a single RJ45 cable. Moreover, this facility for measuring energy consumption in tertiary buildings could be a major advantage, as building owners are required to submit their data to the OPERAT [30] platform set up by ADEME (French Environment and Energy Management Agency) in order to comply with the objectives of the tertiary decree. In this LVDC nanogrid, all the gathered data are ultimately aggregated into an open-source database technology of the influxdb type. A screenshot of the influxdb-v2 interface implemented is shown in Figure 6.

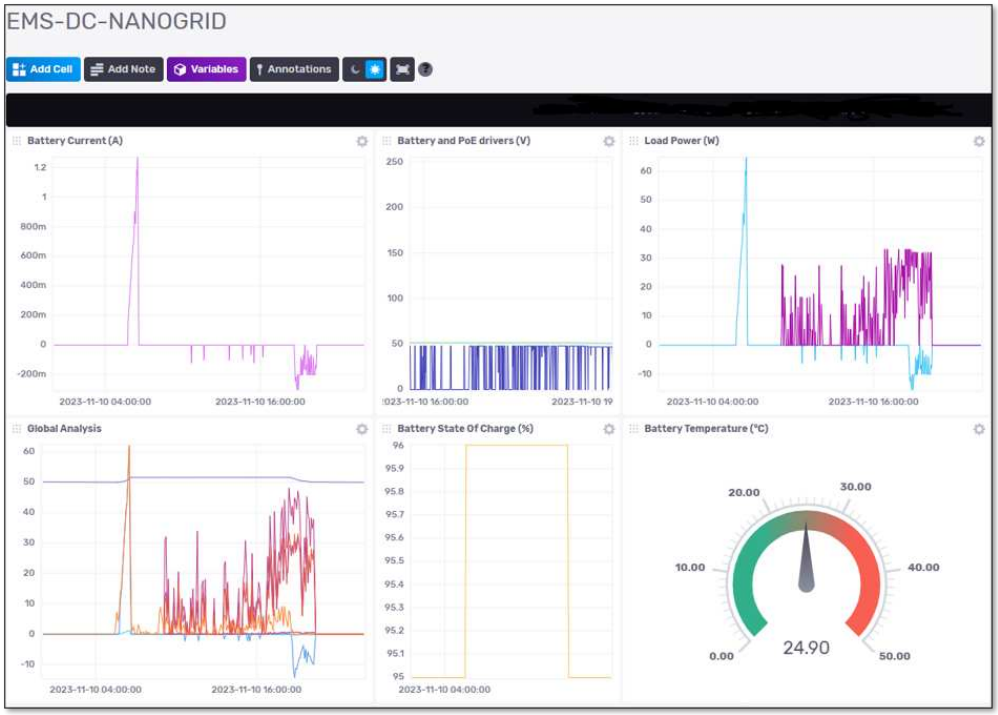

Figure 6. Influxdb-v2 monitoring interface of the nanogrid.

To streamline the analysis of the nanogrid's efficiency, calculations pertaining to the quantification of voltage drops and the overall system efficiency are automated and are displayed on an internally developed monitoring interface within the laboratory.

Preprints.org (www.preprints.org) | NOT PEER-REVIEWED | Posted: 2 February 2024 doi:10.20944/preprints202402.0110.v1

The HMI development, shown in Figure 7 and Figure 8, is carried out using a well-known React.js framework called Next.js. This technology offers serverless capabilities to deliver fast and dynamic web pages. Since this HMI interacts with data, it is essential to pay close attention to its data fetching capabilities. In this regard, Next.js provides built-in functions, making it a wise choice for the given tasks. A specific API was developed to query data directly from InfluxDB within Next.js, ensuring rapid data retrieval, which is vital for real-time energy management dashboards.

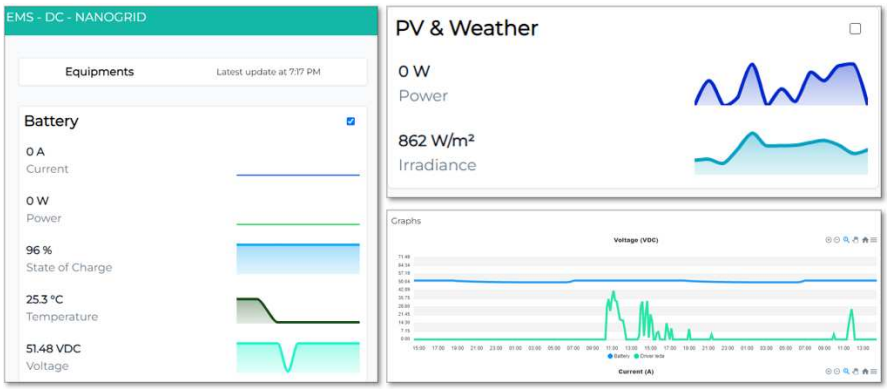

Figure 7. Human Machine Interface - Irradiance (W/m²), Voltage (V), Current (A) and Power (W) monitoring.

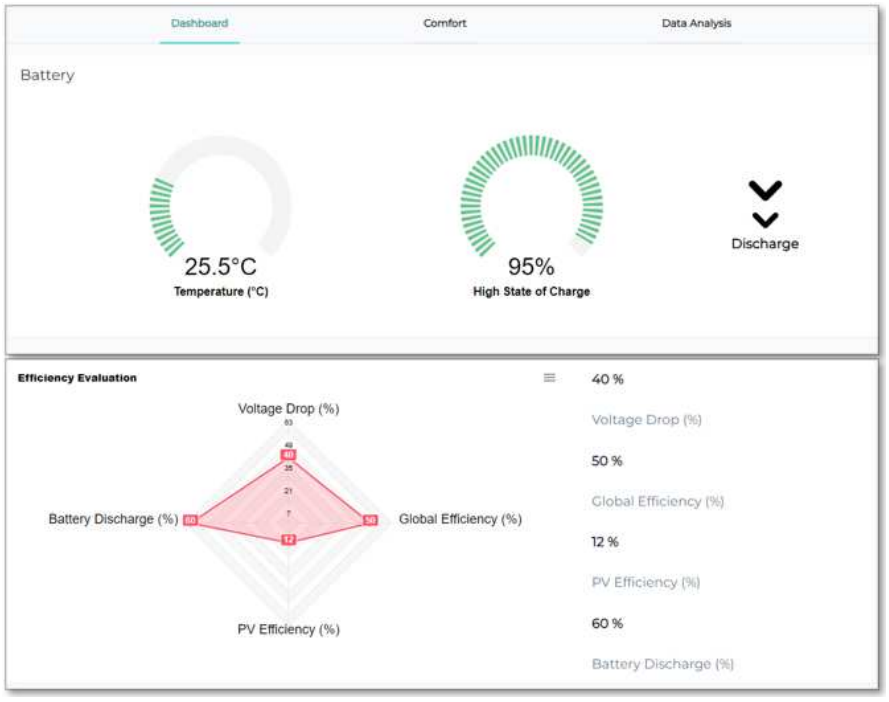

Figure 8. Human Machine Interface - Battery Monitoring and Radar Chart Model for Efficiency Evaluation.

The details of the calculations used to determine the system's efficiency are detailed in the following section.

3. Efficiency Evaluation Methodology

One of the primary constraints in deploying direct current (DC) within buildings pertains to the uncertainty regarding the behavior of DC distribution buses in terms of stability. A significant drop in distribution voltage can lead to degradation of terminal equipment and cause cable overheating,

Preprints.org (www.preprints.org) | NOT PEER-REVIEWED | Posted: 2 February 2024 doi:10.20944/preprints202402.0110.v1

due to the increased current consumption. Regarding the overall efficiency of the system, it would be 100% in the case where the power supplied equals the power consumed. However, Joule losses in the cables and the efficiency of the components inevitably affect the system's performance. Consequently, the objective of this LVDC nanogrid is to reduce energy losses during energy distribution, and the instrumentation carried out in this project aims to quantify its advantages and its limitations. The efficiency measurement was carried out under two scenarios on the nanogrid; in one case where DC/AC and AC/DC converters are integrated into the electrical distribution, and in another case, where the distribution is carried out entirely in 48VDC. The data are extracted from the supervision interface which allows quantifying these elements.

3.1. Voltage drop

The methodology from [23] is employed to quantify the theoretical voltage drops that could occur on the DC bus based on the following calculations. First, the resistance $r(\Omega)$ of the cable is calculated, followed by the percentage (%) of voltage drop. This is based on factors such as distance, cable cross-sectional area, distribution voltage, and the required power :

$$r = \frac{\rho \times 2L}{S} \tag{1}$$

where ρ = 0.01724 Ohm.mm²/m is the copper resistivity, L multiplied per 2 for DC distribution is the distance cable (m), and S is the cable cross-section (mm²). Then the voltage drop $\Delta v\%$:

$$\Delta v\% = \frac{100 \times I \times r}{V} \tag{2}$$

with V the DC bus voltage (V) and I the current (A) used, which is calculated from the final power required. As an example case, the evolution of voltage drop depending on power load demand is plotted in Figure 9 for two different cable cross-sections: 1.5mm² and 2.5mm².

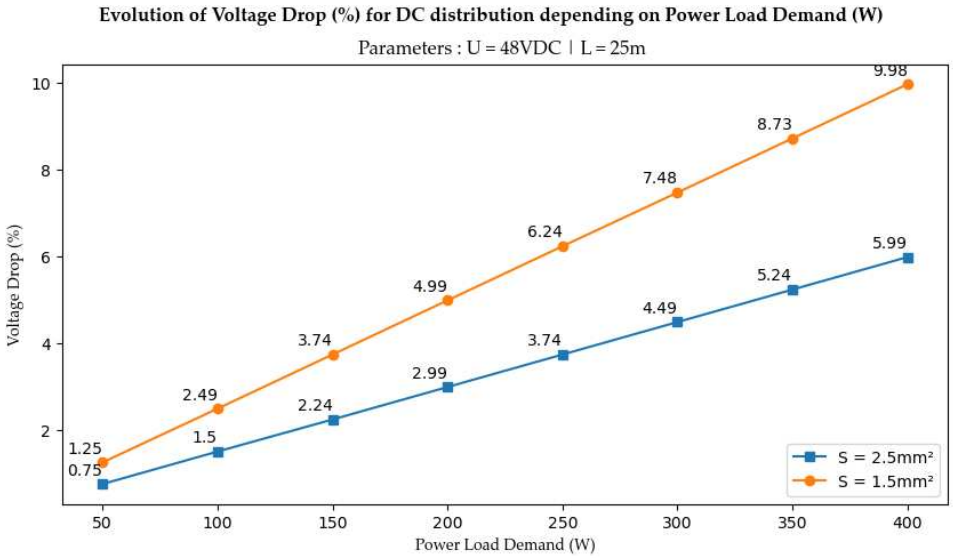

Figure 9. Comparison of voltage drops evolution for 1.5mm² and 2.5mm² cable cross-section.

These two sections are the most commonly used in buildings. The distribution voltage chosen is 48 VDC and the connection distance is 25m. These parameters correspond to the nanogrid deployment described previously. If we refer to the requirements of standard NFC-15100 for low-voltage electrical installations, a voltage drop of less than 3% must be respected for lighting and 5% for other equipment.

 doi:10.20944/preprints202402.0110.v1

Even though this standard applies to AC, we consider that we need to respect the same values in order to offer an architecture that complies with current safety standards. From the curves in Figure 9, it can be seen that theoretically, the 5% value is respected up to 200 W for a 1.5mm² cross-section and around 330 W for 2.5mm² for a wiring distance of 25m at 48 VDC. In order to compare this methodology with experimental values, a test bench and measurement results are presented in section 4.

In the context of direct current (DC) distribution, as the current consumed by the load increases, the voltage drop also increases. Consequently, the total power consumed rises, impacting the nanogrid's energy efficiency. Regarding an electrical distribution including solar energy in line with today's norms, its transitions from direct current to alternating current (AC) by incorporating an inverter and an AC/DC converter. In this case, it's assumed that voltage drops are negligible for an identical cable cross-sectional area because at 230VAC, the current is much less higher. Therefore, the impact on the nanogrid's energy efficiency in this case will depend on the efficiency of the DC/AC and AC/DC converters. In order to establish a comparison between these two kind of deployment, a comparison model is proposed in next subsection.

3.2. Efficiency model

A theoretical efficiency model is established for this study, based on the following fixed parameters and for different points of power demand $Pn(W)$.

3.2.1. Efficiency for DC/AC/DC Distribution

For an assessment of the efficiency of DC/AC/DC distribution, the theoretical system includes a double conversion of current: firstly from DC (produced by the photovoltaic panels or another DC source) to AC (to comply with the current electrical standard in buildings), and secondly from AC to DC for all appliances such as batteries, electronic equipment and LEDs. This is a representation of what currently happens in buildings that receive solar energy and use direct current appliances. This type of installation comprises an inverter, to transform the direct current from the solar panels into standard 230 VAC, and an AC/DC converter, to supply one or more devices with direct current. This study is based on a single distribution line, so it is assumed that there is only one AC/DC converter to supply an appliance with a power rating of 50 to 400W. Figure 10 is a schematic representation of this type of installation.

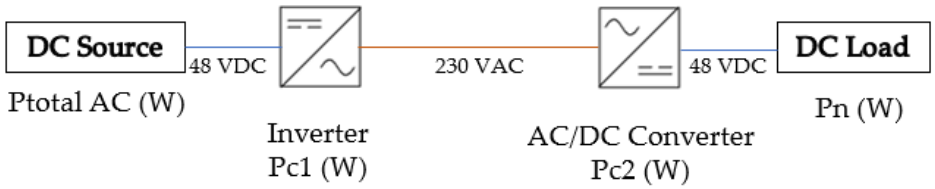

Figure 10. Diagram of a DC/AC/DC distribution corresponding to current installations in buildings.

The system efficiency $\eta th_{AC}(\%)$ is calculated by dividing the end device power consumption $Pn(W)$ by the total power consumed by the system $Ptotal_{AC}(W)$, taking into account the impact of the converters energy consumption, given by the datasheet of the components :

$$\eta th_{AC} = \frac{Pn}{Ptotal_{AC}} \times 100 \tag{3}$$

$$Ptotal_{AC} = Pn + Pc1 + Pc2 \tag{4}$$

 doi:10.20944/preprints202402.0110.v1

with $Pc1$ the inverter power consumption (W) and $Pc2$ the AC/DC converter power consumption (W).

3.2.2. Efficiency for DC Distribution

For a DC distribution efficiency evaluation, the theoretical system hypothesis is that 48VDC voltage is distributed from the source to the final DC appliance, as represented in Figure 11.

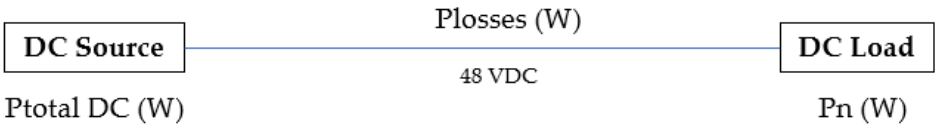

Figure 11. Diagram of a DC distribution corresponding to a end-to-end LVDC Nanogrid.

The system efficiency $\eta th_{DC}(\%)$ is calculated by dividing the power demanded by the end device $Pn(W)$ by the total power consumed by the system $Ptotal_{DC}(W)$, taking into account the impact of voltage drops with $P_{losses}(W)$ as follows :

$$\eta th_{DC} = \frac{Pn}{Ptotal_{DC}} \times 100 \tag{5}$$

$$P_{losses} = (\frac{Pn}{V})^2 \times r \tag{6}$$

$$Ptotal_{DC} = Pn + P_{losses} \tag{7}$$

whith V, the DC bus voltage (V) and r the cable resistance (Ω). The results obtained for $\eta th_{AC}(\%)$ and $\eta th_{DC}(\%)$ are shown in Figure 12.

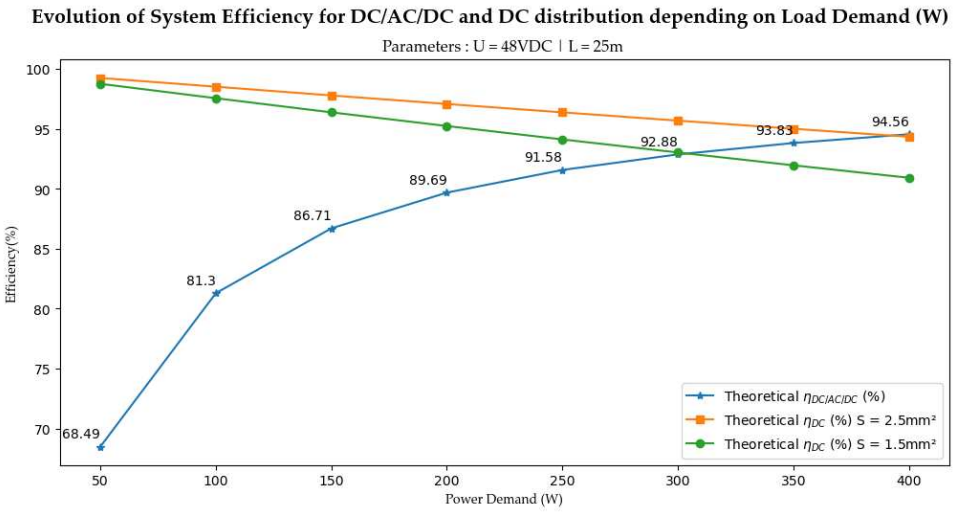

Figure 12. Efficiency model AC vs DC distribution - Comparison for 1.5 and 2.5mm² cable cross-section.

According to the results obtained by the model, a meeting point is obtained between the efficiency of a DC/AC/DC system and a DC system for two different cable cross-sections. For 1.5mm², the maximum power limit is 300 W, because beyond that, 48VDC efficiency becomes lower than AC, and for 2.5mm², the limit is 400 W. However, it doesn't seem wise to consider DC deployments that would aim to get closer to these limits, because if we refer to the results obtained in Figure 9, it can be

 doi:10.20944/preprints202402.0110.v1

seen Figure 12 that although the efficiency is proven to be higher in DC under these conditions, the theoretical voltage drops would be out of the norm if we're close to maximum power limit : higher than 7% for 1.5mm² and higher than 6% for 2.5mm².

As the aim of this model is to be generic, input parameters such as DC bus voltage or wiring distance can be modified to give a different meeting point between the efficiency of the two systems. To illustrate these theoretical values, the following section presents the test bench set up to provide experimental values for the established hypotheses.

4. Results and Discussion

4.1. Experimental testbench

To quantify the reliability of the theoretical model, an experimental test bench is set up on the nanogrid whose diagram is represented in Figure 13.

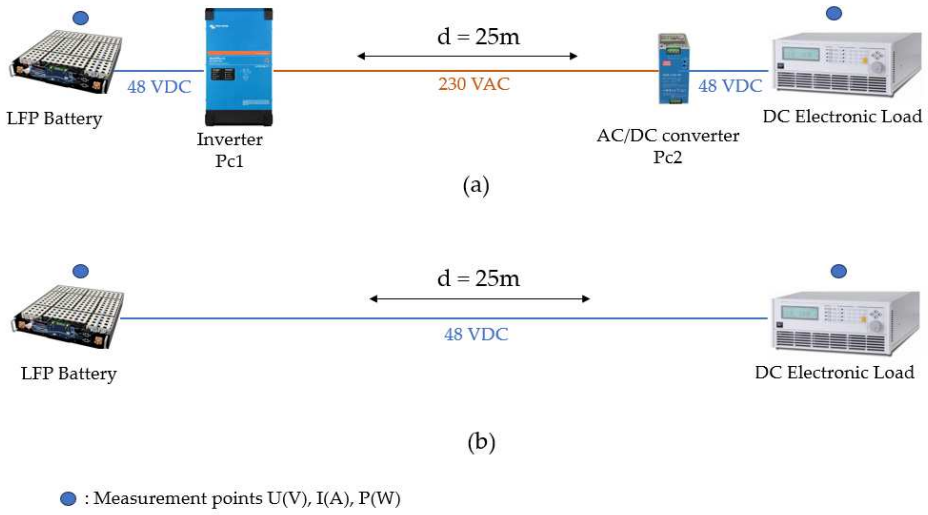

Figure 13. Testbench setup for DC/AC/DC distribution (a) and for DC distribution (b).

The blue dots on the diagram represent the following measurement points : current (A), voltage (V) and power (W). These measurements are carried out by the DC electronic load and the battery. Both of them has its own internal components for taking these measurements. The battery transmits its data using the Victron API and the programmable load can communicate via a serial link or IP network. As all the equipment is connected as described in Figure 5, the measurement data is entered directly into the database. Measurements were carried out with 3G1.5mm² and 3G2.5mm² cable, each 25m long, to represent actual nanogrid deployment on the company's premises. The LFP battery is used as an energy source, as solar energy is intermittent, and it would have been inappropriate to compare two measurements taken at different times, as sunshine levels would not have been exactly the same. The DC electronic load is used to simulate a load from 50 to 400W. All the equipment references and their parameters are listed in Table 1, according to manufacturer data. Next sections present the experimental measurement obtained on the testbench.

Table 1. List of references and parameters of the components used for the experimental test bench.

Equipment	Reference	Power consumption (W)
Battery	PYLONTECH US2000C	-
Inverter	MULTIPLUS-II VICTRON	18 W
AC/DC converter	NDR-240-48 MEANWELL	5 W
DC Electronic load	CHROMA 63800	1.8 kW max

 doi:10.20944/preprints202402.0110.v1

4.2. Comparison between DC/AC/DC and 48 VDC distribution for a cable cross-section of 1.5mm²

Figure 14a compares the experimental efficiency curves of the DC/AC/DC and DC distributions for a 1.5mm² cross-section and a distance of 25m. From the experimental measurements, it can be seen that efficiency is 40.8% higher with 48VDC for a power demand of 50W than with a DC/AC/DC system. For a load of 100W, the efficiency is 23% higher than in DC/AC/DC. The experimental power limit identified under these conditions is around 270W, because beyond this point, DC/AC/DC efficiency is higher. It should be noted that the voltage drops measured experimentally ranged from 2.59% for 50W to 12.8% for 250W, as shown in Figure 14b. In order to comply with NFC15-100 standards, for example, the final power should not exceed 100W for these conditions (25m at 48VDC), in order to respect 5% voltage drop. This result is consistent with a similar study of K. Hafsi et al [31] that measured the 802.3bt standard: for a distance of 100m, line losses were 20%. This confirms that DC deployments need to be studied on a case-by-case basis, as many parameters will influence the efficiency of the installation, such as: cabling distance, final power and equipment quality.

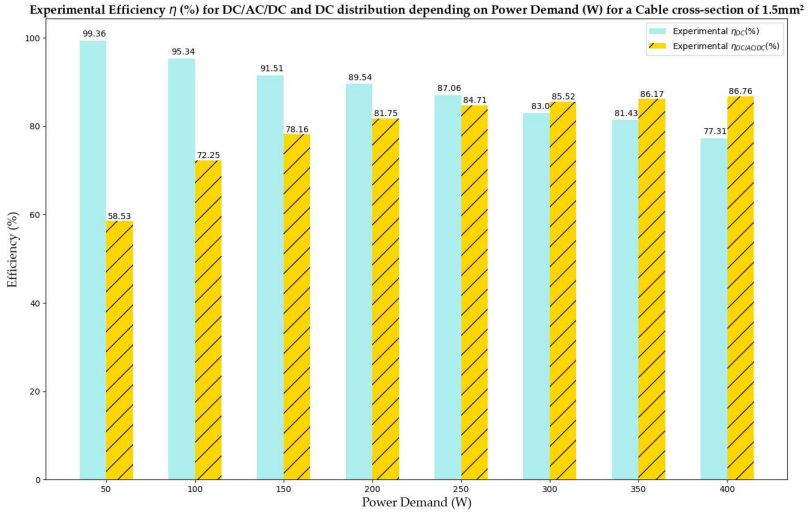

(a)

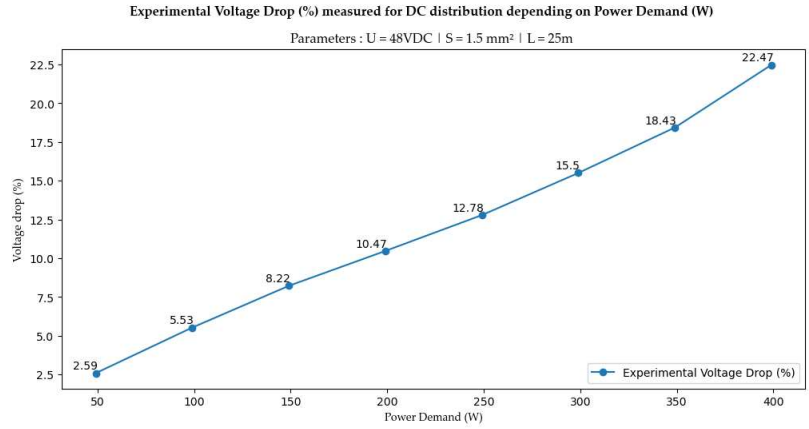

(b)

Figure 14. For a 1.5mm² cable cross-section, comparison of efficiency η (%) measured for DC and DC/AC/DC distribution (a), and evolution of experimental voltage drop (%) measured for DC distribution (b).

The discrepancy with the theoretical voltage drops calculated in Figure 9 can be explained by several factors : the internal resistances of the battery and programmable load, cable quality, connector resistances and protection elements. This also means that special care must be taken during installation,

 doi:10.20944/preprints202402.0110.v1

and measurements must be carried out in addition to theoretical calculations. This additional check would verify that voltage drops are respected and that the installation complies with current standards, in order to avoid any safety risks for users and damage to terminal equipment. In the case of the nanogrid deployment described in this paper, where the terminal loads are LEDs and DC fans with a maximum power demand of 40W, the experimental efficiency has been measured to be 41% more efficient than a conventional DC/AC/DC system.

4.3. Comparison between DC/AC/DC and 48 VDC distribution for a cable cross-section of 2.5mm²

A second comparison of the nanogrid efficiency for DC/AC/DC or DC distribution is made with a 2.5mm² cross-section, and the results are shown in Figure 15a. As expected, DC efficiency is higher up than DC/AC/DC to around 400W. At low power levels (below 50W), the efficiency gain is not much higher than with 1.5mm², so it may be more cost-effective to use 1.5mm² for DC appliances which do not require supply power superior to 50W. This power value concerns appliances like lighting, televisions, rechargeable electronics, security systems and some computers [32]. Furthermore, this result confirms that the cable cross-section necessary to use the IEEE 802.3bt standard remains effective and there is no need to modify the installation parameters to gain efficiency, such as using a section of cable higher.

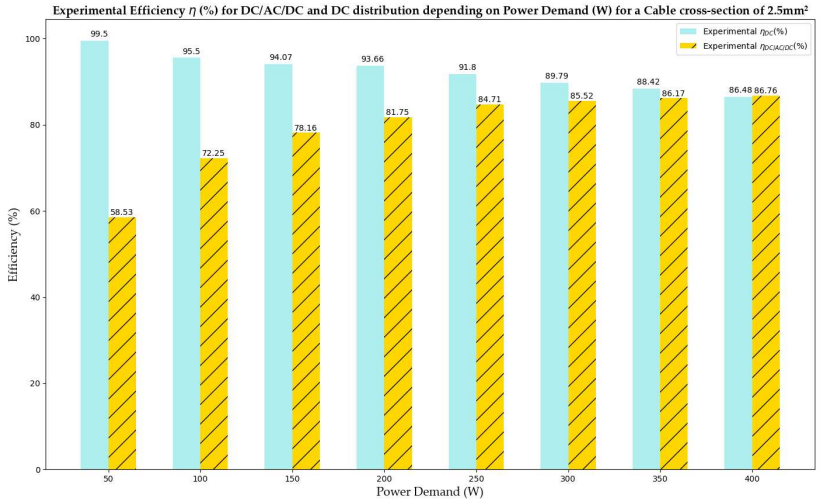

(a)

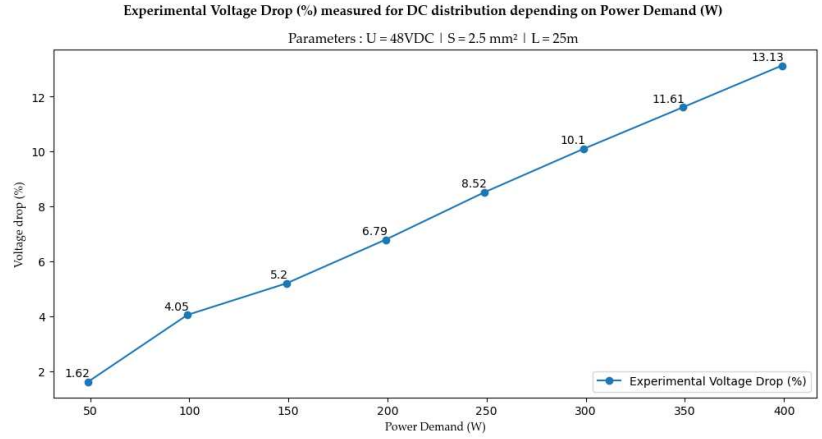

(b)

Figure 15. For a 2.5mm² cable cross-section, comparison of efficiency η (%) measured for DC and DC/AC/DC distribution (a), and evolution of experimental voltage drop (%) measured for DC distribution (b).

 doi:10.20944/preprints202402.0110.v1

Concerning voltage drops shown in Figure 15b, the same phenomenon is observed than with 1.5mm² section : measured voltage drops were higher than expected. A voltage drop of 1.62% for 50W up to 13% for 400W is measured, instead of the theoretical 0.75% and 6% expected in (Figure 9). These results mean that although DC efficiency is higher up than DC/AC/DC to the value of 400W, the power limit for 25m distance respecting voltage drops at 5% would therefore be 150W, for this cable cross-section.

As a perspective, these results indicate that it would be wise to combine higher voltage levels in DC buildings, such as 400 VDC for example, in order to minimize the distances for 48 VDC distribution. Thus, this combination of high and low voltage would make it possible to use a voltage lower than 120 VDC as close as possible to users. This electrical distribution would therefore be included in the secure "very low voltage" voltage range.

5. Conclusions

In this study, the deployment of an end-to-end 48VDC nanogrid in a real-world enterprise is demonstrated and investigated. The nanogrid includes solar PV, LFP battery storage and end devices powered via PoE 802.3bt for a distance of 25m. To quantify the efficiency and limits of the LVDC nanogrid compared to a conventional photovoltaic installation using 230VAC, an experimental test bench is set up, measurements are taken and compared to the theoretical results calculated before the experiment. The efficiency of the DC nanogrid is measured to be 40% higher than a conventional DC/AC/DC installation for a final load of 50W and 23% higher for a final load of 100W. This result is significant for potential energy gains in buildings. Indeed, over distances less than 100m and low powers, it is confirmed that direct current makes it possible to optimize electrical architectures. In the case of this work, the 48VDC voltage was studied for its compatibility with numerous electrical devices and particularly the IEEE 802.3bt standard. It has been demonstrated that the 802.3bt standard can be used in innovative ways on devices other than IT equipment, such as lighting or DC fans. A challenge lies in the fact that a standard DC distribution voltage could be defined so that DC terminal equipment is standardized to this voltage and facilitate their installation. To know the limitations of DC compared to a DC/AC/DC installation in other deployment conditions, the novel methodology presented in this article can be reproducible by changing input parameters such as voltage, cable distance, cable cross-sections and converter efficiency. This methodology can thus be used as a design tool when deploying nanogrids. As a perspective, the notions of costs could be integrated in order to obtain a technico-economic assessment in the building design phase. Finally, similar tests could be carried out with different cable qualities in order to check whether there would be quantitative improvements regarding voltage drops.

Author Contributions: Conceptualization, O.G, D.G.-C.,F.A., P.-O.L.D.P.; methodology, O.G.; software, O.G. and F.B.; validation, D.G-C, F.A., P.-O.L.D.P, J.-P.C.; formal analysis, O.G.; investigation, O.G..; resources, O.G.; writing—original draft preparation, O.G.; writing—review and editing,O.G., D.G-C, F.A., P.-O.L.D.P, J.-P.C.; visualization, O.G. and F.B.; supervision, D.G-C, F.A., P.-O.L.D.P,L.L., J.-P.C.; project administration, L.L. and J.P.C. All authors have read and agreed to the published version of the manuscript.

Funding: This research is funded by the National Association of Research and Technology (ANRT), the company Intégrale Ingénierie, the University of La Réunion and the University of Grenoble-Alpes.

References

1. French government. Tertiary decree n°2019-771, *JORF n°0171*. 2019.
2. French government. Building Automation and Control System (BACS) decree n°2020-887. *JORF n°0177*. 2020.
3. French government. Law n° 2015-992 of August 17, 2015 on the energy transition for green growth. *JORF n°0193 of 19th august 2015*. 2015.
4. Energy observatory SPL Horizon Réunion. Balance sheet energy of La Réunion 2020. Available online : https://energies-reunion.com/nos-actions/observation/ (accessed on 15 January 2024).

5. Open Data EDF Réunion, Available online : https://opendata-reunion.edf.fr/ (accessed on 15 January 2024).
6. Burmester, D. A review of nanogrid topologies and technologies. *Renewable and Sustainable Energy Reviews*, **2017**.
7. Glasgo, B.;Azevedo, I.;Hendrickson, C. How much electricity can we save by using direct current circuits in homes? Understanding the potential for electricity savings and assessing feasibility of a transition towards DC powered buildings. *Applied Energy*.**2016**, *180*.
8. Gerber, D.; Liou, R.; Brown, R. Energy-saving opportunities of direct-DC loads in buildings. *Applied Energy*. **2019**, *248*.
9. Chauhan, R. K.; Rajpurohit, B. S. DC distribution system for energy efficient buildings. In Proceedings of the 2014 Eighteenth National Power Systems Conference (NPSC), Guwahati, India, 2014, pp. 1-6.
10. Alsaedi, A.; Alharbi, F.; Alahdal, A.; Alahmadi, A.; Ammous, A.; Ammous, K. Low Voltage Direct Current Supplies Concept for Residential Applications. *Energy Exploration & Exploitation*. **2022**,*40(3)*,1078-1097.
11. Manandhar, U.; Ukil, A.; Kiat Jonathan, T. K. Efficiency comparison of DC and AC microgrid. In Proceedings of the 2015 IEEE Innovative Smart Grid Technologies - Asia (ISGT ASIA), Bangkok, Thailand, 2015, pp. 1-6.
12. Ammous, A.; Alsaedi, A.; Alahmadi, A. N. M.; Alharbi, F.; Ammous, K. Efficiency Performances of LVDC Supplies for Residential Building.*Computer Systems Science and Engineering*. **2023**, *45*.
13. Ollas, P.; Thiringer, T.; Persson, M.; Markusson, C. Energy Loss Savings Using Direct Current Distribution in a Residential Building with Solar Photovoltaic and Battery Storage. *Energies* **2023**, *16*, 1131.
14. Vossos, V.; Garbesi, K.; Shen, H. Energy savings from direct-DC in U.S. residential buildings. *Energy and Buildings*. **2014**, *68*, Part A.
15. Chacko, R.; Thevarkunnel, A.; Lakaparampil, Z.V.; Thomas, J. DC nanogrid for Buildings: Study based on experimental investigation of load performance and Annual energy consumption. *Materials Today: Proceedings*. **2022**, *58*, Part 1.
16. Living Energy Farm, Available online : https://livingenergyfarm.org/energy/ (accessed on 15 January 2024).
17. Glasgo, B.; Lima Azevedo, I.; Hendrickson, C. Expert assessments on the future of direct current in buildings. *Environmental Research Letters*. **2018**, *13*.
18. Antoniou, D.; Tzimas, A.; Rowland Simon M. Transition from alternating current to direct current low voltage distribution networks. *IET Generation, Transmission & Distribution*. **2015**, *9*.
19. Dastgeer, F. Gelani, H. E.; Anees, H. M.; Paracha, Z. J.; Kalam, A. Analyses of efficiency/energy-savings of DC power distribution systems/microgrids: Past, present and future. *International Journal of Electrical Power & Energy Systems*. **2019**, *104*.
20. Gelani, H.E.; Dastgeer, F.; Nasir, M.; Khan, S.; Guerrero, J.M. AC vs. DC Distribution Efficiency: Are We on the Right Path? *Energies* **2021**, *14*, 4039.
21. Beretta, D.; Mocoteguy, P.; Sessa, G.; Limagne, M.; Boucher, J.-E. A 100% renewable isolated microgrid in Mafate. In Proceedings of the CIRED 2018 Ljubljana Workshop on Microgrids and Local Energy Communities, 2018.
22. Abbezzot, C.; Francou, J.; Calogine, D. Demand side management applied to a standalone microgrid. *International Journal of Smart Grid and Clean Energy*. **2022**, *11* (4), pp.127-134.
23. Moussa, S.; Ghorbal, M.J.-B.; Slama-Belkhodja, I. Bus voltage level choice for standalone residential DC nanogrid. *Sustainable Cities Society*. **2019**, *46*, 101431.
24. Habibi, S.; Rahimi, R.; Ferdowsi, M.; Shamsi, P. DC Bus Voltage Selection for a Grid-Connected Low-Voltage DC Residential Nanogrid Using Real Data with Modified Load Profiles. *Energies* **2021**, *14*, 7001. https://doi.org/10.3390/en14217001
25. Richard, L.; Boudinet, C.; Ranaivoson, S.A.; Rabarivao, J.O.; Befeno, A.E.; Frey, D.; Alvarez-Hérault, M.-C.; Raison, B.; Saincy, N. Development of a DC Microgrid with Decentralized Production and Storage: From the Lab to Field Deployment in Rural Africa. *Energies* **2022**, *15*, 6727. https://doi.org/10.3390/en15186727
26. Ore, J.; Groll, A. E.; Design and Development of a Decentralized and Distributed IoT Home Monitoring System Within a DC Nanogrid. In Proceedings of the 2020 Building Performance Analysis Conference and SimBuild co-organized by ASHRAE and IBPSA-USA, September 29 – October 1, 2020.
27. Uddin, M.; Mo,H.; Dong,D.; Elsawah,S.; Zhu, J.; Guerrero, J. M. Microgrids: A review, outstanding issues and future trends.*Energy Strategy Reviews*.**2023**,*49*.

 doi:10.20944/preprints202402.0110.v1

28. Liu, Z.; Li, M. Research on Energy Efficiency of DC Distribution System. *AASRI Procedia*, **2014**, *7*, Pages 68-74.
29. IOS-net, Available online : https://galilee.univ-reunion.fr/ (accessed on 15 January 2024).
30. OPERAT platform, Available online : https://operat.ademe.fr/ (accessed on 15 January 2024).
31. Hafsi, K.; Genon-Catalot, D.;Thiriet, J. -M.;Lefevre,O. DC building management system with IEEE 802.3bt standard. In Proceedings of the 2021 IEEE 22nd International Conference on High Performance Switching and Routing (HPSR), Paris, France, 7-10 June 2021;pp. 1-8.
32. Garbesi, K.; Vossos, V.; Shen, H. Catalog of DC Appliances and Power Systems. *Lawrence Berkeley National Laboratory*. **2012**.